Since January 2020 Elsevier has created a COVID-19 resource centre with free information in English and Mandarin on the novel coronavirus COVID-19. The COVID-19 resource centre is hosted on Elsevier Connect, the company's public news and information website.

Virus Research 151 (2010) 213–219

Contents lists available at ScienceDirect

Virus Research

journal homepage: www.elsevier.com/locate/virusres

APOBEC3G directly binds Hepatitis B virus core protein in cell and cell free systems

Dongjiu Zhao[a,b], Xianfeng Wang[b], Guohua Lou[b], Guoping Peng[b], Jie Li[b], Haihong Zhu[b], Feng Chen[b], Shuping Li[b], Dongcheng Liu[b], Zhi Chen[b], Zhenggang Yang[b,*]

[a] Department of Anatomy, School of Medicine, Zhejiang University, Hangzhou 310058, PR China
[b] Institute of Infectious Diseases, State Key Laboratory for Diagnosis and Treatment of Infectious Diseases, the First Affiliated Hospital, School of Medicine, Zhejiang University, 79 Qingchun Road, Hangzhou 310003, Zhejiang Province, PR China

ARTICLE INFO

Article history:
Received 18 March 2010
Received in revised form 13 May 2010
Accepted 18 May 2010
Available online 25 May 2010

Keywords:
APOBEC3G
HBV core protein
Fluorescence resonance energy transfer
Surface plasmon resonance
RNA

ABSTRACT

APOBEC3G (A3G) is an intrinsic antiretroviral factor which can inhibit Hepatitis B virus (HBV) replication. This antiviral activity mainly depends on A3G incorporation into viral particles. However, the mechanisms of A3G packaging into HBV particles have not been well characterized. In this paper, we demonstrated that A3G interacted with the HBV core protein (HBc) directly in co-transfected HepG2 cells using the fluorescence resonance energy transfer (FRET) approach. In addition, we further found that this interaction did not require other factors *in vitro* using surface plasmon resonance (SPR) technology on BIAcore 3000. While cellular RNA or viral RNA was added to A3G protein solution before flow through the BIAcore chip, the interaction was not affected. In conclusion, these results suggest the possibility that A3G is incorporated into HBV viral particles via direct binding with HBc protein.

1. Introduction

Hepatitis B virus (HBV) afflicts more than 350 million individuals world-wide, and causes acute and chronic viral hepatitis that in many cases lead to subsequent liver cirrhosis and emergence of hepatocellular carcinoma (Kao and Chen, 2002). To date, interferon and nucleotide analogues are the approved treatments for chronic HBV infection, but the side effects and drug resistance limit the use of these available options. The further development of potential antiviral therapy is still required.

Cellular APOBEC (apolipoprotein B mRNA-editing enzyme catalytic polypeptide 1-like) is a family of cellular cytidine deaminase-editing enzymes, including APOBEC1, APOBEC2, seven APOBEC3 variants and activation-induced deaminase (Aguiar and Peterlin, 2008; Jarmuz et al., 2002; Wedekind et al., 2003). APOBEC3G (A3G) belongs to this family and has potent antiretroviral activity (Mangeat et al., 2003; Turelli et al., 2004; Wang and Wang, 2009). A3G contains a duplication of the conserved HXEX23–28-CPX2–4C motif, wherein the N-terminal domain probably has an ability to bind to RNA, while the C-terminal domain possesses cytidine deamination activity (Chiu and Greene, 2008). Previous studies have suggested that the deamination of cytidine to uridine in nascent minus-strand transcripts during reverse transcription is the most important reason for A3G's antiviral effects (Harris et al., 2003; Mangeat et al., 2003). However, recent data have shown that A3G can inhibit HBV replication in a deaminase-independent way (Nguyen et al., 2007; Turelli et al., 2004). In the absence of viral infectivity factor (Vif), A3G is specifically incorporated into the assembling HIV-1 virions, reducing the infectivity of the newly produced virus (Alce and Popik, 2004). It is also incorporated into murine leukemia viruses and coronaviruses (Wang and Wang, 2009; Zhang et al., 2008). The mechanism of A3G incorporating into HIV-1 virons may be through interaction with HIV-1 Gag (Cen et al., 2004; Douaisi et al., 2004). Recently, some reports pointed out that A3G virion recruitment by Gag/NC is RNA-dependent (Burnett and Spearman, 2007; Wang et al., 2008b), while others believed that it was RNA-independent (Alce and Popik, 2004; Soros et al., 2007). Whether cellular RNA or viral genomic RNA plays a role in the virion packaging of A3G remains to be determined.

The HBV genome is a small, circular and partly double-stranded DNA of about 3.2 kb in length. During HBV infection, the relaxed circular (RC)-DNA is converted to covalently closed circular DNA (cccDNA), which acts as the template for transcription of pregenomic RNA (pgRNA) and antigen-coding mRNAs. pgRNA is the template for reverse transcription and specifies the codes for the HBV core protein (HBc) and the HBV polymerase. HBc is the major component of the nucleocapsid shell packaging the HBV genome. Furthermore, it plays an essential role in the formation of HBV

* Corresponding author. Tel.: +86 0571 87236579; fax: +86 0571 87068731.
E-mail address: yangzg@zju.edu.cn (Z. Yang).

0168-1702/$ – see front matter © 2010 Elsevier B.V. All rights reserved.
doi:10.1016/j.virusres.2010.05.009

replication complexes (Guarnieri et al., 2006). Baumert et al. (2007) mentioned that A3G did not affect the early steps of the HBV life cycle, but it may interfere with the packaging of HBV. However, the mechanism by which A3G is incorporated into HBV viral particles has not been fully established.

To further explore the relationship between A3G and HBc, fluorescence resonance energy transfer (FRET) was performed in HepG2 cells and surface plasmon resonance (SPR) measurement was carried out in cell free condition. To investigate whether RNA affects the A3G–HBc interaction, cellular RNA or virus RNA was added to the A3G protein solution before flow through the SPR chip. We demonstrate that A3G can directly bind to the HBc protein, and that the binding is not dependent on RNA.

2. Materials and methods

2.1. Plasmids

HBc coding sequence was amplified by PCR from pZ1.3 (1.3 copies HBV genome), while A3G was amplified by PCR using wild-type pcDNA-APO3G as the template. HBc or A3G was then inserted into *Hin*dIII/*Kpn*I restriction sites of pEYFP-N1 or pECFP-N1 (Clontech), resulting in pHBc-YFP and pA3G-CFP. The pECFP–YFP vector which contains CFP–15-amino acid-linker–YFP was used as a positive control. A3G with a haemagglutinin (HA) tag at the C-terminus (A3G-HA) was constructed by cloning A3G into the *Hin*dIII and *Eco*RI restriction sites of pcDNA3.1 (+). To construct an assembly defective mutant of HBc, Y132A mutation was completed using overlap extension PCR (Hu et al., 2009) and taking pZ1.3 as template. The final PCR products of HBc-Y132A-HA were digested with *Hin*dIII/*Eco*RI and inserted into pcDNA3.1 (+) to yield pHBc-Y132A-HA. All recombinant plasmids were extracted using Plasmid mini-prep kit (Qiagen) and confirmed by sequencing.

2.2. Cell culture and transfection

A hepatoma cell line (HepG2) and a human embryonic kidney cell line (HEK-293T) were maintained in DMEM containing 10% fetal bovine serum. The HBV-expressing stable cell line (HepG2.2.15) was cultured in DMEM containing 10% fetal bovine serum and 200 μg/mL G418. For confocal microscopy and FRET experiments, HepG2 cells (2×10^5/well) were seeded on coverslips in 6-well tissue culture plates, and cultured overnight at 37 °C. The cells were then transfected with the appropriate plasmids using Lipofectamine 2000 (Invitrogen) according to the manufacturer's protocol.

2.3. Western blot analysis

Cells were seeded in 6-cm culture dish and obtained 48 h after transfection. Cells were washed twice with PBS and resuspended, then mixed with an equal volume of cell lysis buffer (20 mM Tris, pH 7.5, 150 mM NaCl, 1% Triton X-100, 2.5 mM sodium pyrophosphate, 1 mM EDTA, 1% Na_3VO_4, 0.5 μg/mL leupeptin, and 1 mM phenylmethanesulfonyl fluoride). The cell lysates were denatured and reduced by adding 5× SDS-PAGE sample buffer followed by boiling at 100 °C for 5 min. Protein was resolved by 10% SDS-PAGE and transferred onto nitrocellulose membranes (Amersham Biosciences). CEM15 (A3G) purified mouse monoclonal antibody (SD30806C) was obtained from Abgent Company, USA and HBc monoclonal antibody (C8A033M) was purchased from Biodesign, USA. Each protein was detected with a corresponding primary antibody. The blotting signal was visualized by enhanced chemiluminescence (ECL; Pierce).

2.4. FRET imaging

HepG2 cells were transfected with plasmids encoding CFP and YFP fusion proteins and observed in extracellular medium which was composed of: 150 mM NaCl, 5 mM KCl, 2 mM $CaCl_2$, 1 mM $MgCl_2$, 10 mM HEPES, and 10 mM glucose at pH 7.3 with Tris base. The three-cube FRET measurement has been described previously (Gao et al., 2007). Images were obtained with an inverted microscope Nikon TE2000 equipped with a mercury lamp light source (100 W), Dual-View (Optical Insights, LLC, Santa Fe, NM) and a SNAP-HQ-cooled CCD camera. Three-cube FRET filter cubes were listed as follows (excitation, dichroic, emission): CFP (S430/25 nm; 455dclp; S470/30 nm), YFP (S500/20 nm, Q515lp, S535/30 nm), and FRET (S430/25 nm, 455dclp, S535/30 nm). We used binning 2×2 modes and 200 ms of exposure time. Average background signal was determined as the mean fluorescence intensity from a blank area and was subtracted from the raw images before carrying out FRET calculations. The following equation was used to calculate the FRET ratio (FR): $FR = [FRET - (b \times CFP)]/(a \times YFP)$, in which parameters a and b represent the fractions of bleed-through of YFP and CFP fluorescence through the FRET filter channel, respectively (Takanishi et al., 2006). MetaMorph5.0 software (Universal Imaging, West Chester, PA) was used to control the imaging setup and analyze the cell image data.

2.5. Imaging and acceptor photobleaching

Cells were cultured on glass coverslips for 2 days after transfection. The cells were then rinsed three times in PBS and fixed for 15 min in freshly prepared 4% formaldehyde (Sigma) at room temperature. After washing three more times with PBS, the cells were mounted on slides with 75% glycerol–PBS. Images were obtained with 40× NA 1.0 oil immersion objective lens of a confocal microscopy (FV1000, Olympus). CFP and YFP fluorophore were excited by 458- and 514-nm laser lines at 25-mW argon laser. Band pass filters of 462–484 and 580–612 nm were used in collecting emission from CFP and YFP, respectively. For acceptor photobleaching, images were obtained in the CFP and YFP channels; then a region of cell was selected and the intensity of the signal was calculated. YFP was then selectively photobleached in the defined region of the cell. A second set of images was then obtained using the same conditions prior to photobleaching. The increase in CFP fluorescence after YFP photobleaching corresponds to the original amount of energy transferred from CFP to YFP; thus, the difference in CFP fluorescence before and after photobleaching corresponds to the level of FRET. Effective FRET ratio (E_{EFF}) between CFP (donor) and YFP (acceptor) was quantified with acceptor photobleaching methods (Karpova et al., 2003) using the following equation: $E_{EFF} = ((A_1 - A_0)/A_0) \times 100\%$, in which A_0 and A_1 are the intensities of CFP in the photobleached region before and after photobleaching, respectively.

2.6. Purification of recombinant protein A3G-HA and HBc-Y132A-HA

HEK-293T cells were grown in 10-cm dishes and transfected with pA3G-HA or pHBc-Y132A-HA plasmids by Lipofectamine 2000 (Invitrogen). After 48 h, cells were harvested and HA-fusion proteins were purified by EZviewä Red Anti-HA Affinity Gel (Sigma, E6779) according to the instructions. In brief, cells were lysed in 750 μL lysis buffer (25 mmol/L Tris, 225 mmol/L NaCl, 1% Triton X-100, 1 mmol/L DTT, 10% glycerol, 10 mmol/L NaF, 1 mmol/L Na_2VO_4 and protease inhibitor) and mixed with Anti-HA Affinity Gel beads. Vortex briefly and incubate with thorough, gentle mixing for 1 h at 4 °C. Wash the beads pellet three times by 750 μL lysis buffer. The bound protein was eluted with 100 μg/mL solution of HA-

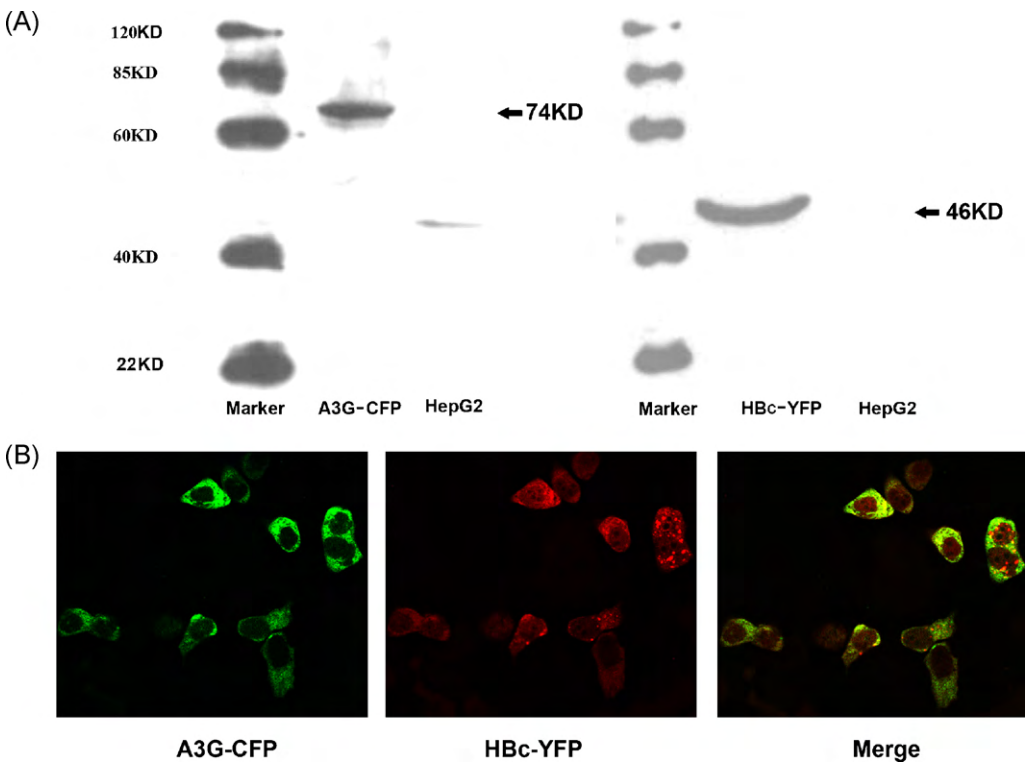

Fig. 1. Co-localization of A3G and HBc in HepG2 cells. (A) Proteins were visualized by western blotting using CEM15 monoclonal antibody or HBc antibody, respectively. (B) Confocal fluorescence imaging of HepG2 cells transfected with A3G-CFP (left), HBc-YFP (middle) and merged (right).

peptide (Sigma, I2149) in 50 μL lysis buffer. The eluting protein was detected by western blot with HA-Tag (6E2) Mouse mAb (Cell Signaling, #2367). The remainder was stored at −70 °C for subsequent protein–protein interaction experiments.

2.7. RNA extraction

HepG2.2.15 can produce not only all of the particles but also a number of replicative intermediates that probably represent recircularized, cccDNA, and single-stranded HBV DNA (Sells et al., 1987). Here these cells were used as a source of viral RNA. Total cellular RNA was extracted from HepG2 and HepG2.2.15 cells, respectively, using the RNeasy RNA extraction kit (QIAGEN, Valencia, CA). The RNAs were quantified by spectrophotometric A260 readings.

2.8. Surface plasmon resonance (SPR) analysis

In our experiments, all analyses of interaction between A3G and HBc in cell free systems were performed on BIAcore 3000 optical biosensors equipped with research-grade CM5 sensor chips (BIAcore AB, Uppsala, Sweden). The chip was pretreated with three injections of 5 μL 50 mM NaOH at a flow rate of 30 μL/min. The sensor surface was activated with a freshly mixed solution of 0.2 M 1-ethyl-3-(3′-dimethylamino-propyl) carbodiimide hydrochloride and 0.05 M N-hydroxysuccinimide for 7 min at a flow rate of 5 μL/min. For immobilization of proteins, the purified HBc-Y132A-HA protein was injected in 100 μL of 10 mM sodium acetate (flow rate: 10 μL/min). After immobilization, each surface was blocked by 1 M ethanolamine at pH 8.5 for 6 min. In order to continuously monitor the non-specific background binding of samples to the carboxymethyl dextran substrate, a control flow cell was pre-activated and immediately blocked with ethanolamine without exposure to HBc-Y132A-HA protein. Then purified A3G protein (140.8 μM) was injected using the KINJECT at a flow rate of 10 μL/min for 180 s, regenerated for 10 s using 50 mM NaOH at a flow rate of 30 μL/min, and then stabilized for 5 min before the next injection. To eliminate the influence of HA-peptide, 100 μg/mL HA-peptide was injected. Progranulin (PGRN, 0.5 μg/μL) was injected as a negative control in the same condition. The interaction analyses were carried out in PBS buffer at 25 °C. Data were analyzed with BIA evaluation 3.1 software (BIAcore).

3. Results

3.1. Co-localization of A3G and HBc in HepG2 cells

The genes encoding A3G and HBc were cloned into pECFP-N1 and pEYFP-N1 expression vectors, named as pA3G-CFP and pHBc-YFP respectively. Plasmids expressing fluorescent fusion proteins were prepared and transiently transfected into HepG2 cells. A3G-CFP and HBc-YFP fusion proteins can be specifically identified by monoclonal antibodies (Fig. 1A).

Next, the localization of the A3G-CFP and HBc-YFP fusion proteins was detected in co-transfected HepG2 cells by confocal fluorescence microscopy. As shown in Fig. 1B, very bright and punctuated A3G-CFP was observed in the cytoplasm while HBc-YFP was not only distributed evenly in the cytoplasm, but also in the nucleus. 240 cells were counted, about 63.3% of the transfected cells were stained positive for HBc predominantly in the cytoplasm, while about 37.7% of the transfected cells displaying both in the nuclei and cytoplasm. This result was consistent with previous reports (Liao and Ou, 1995; Ning and Shih, 2004; Sureau et al., 1986; Wichroski et al., 2006). Meanwhile, about 85.2% of cells co-expressed A3G and HBc, and in a number of co-expressing cells, extensive co-localization was observed. The co-localization raises the intriguing possibility that there is interaction between them.

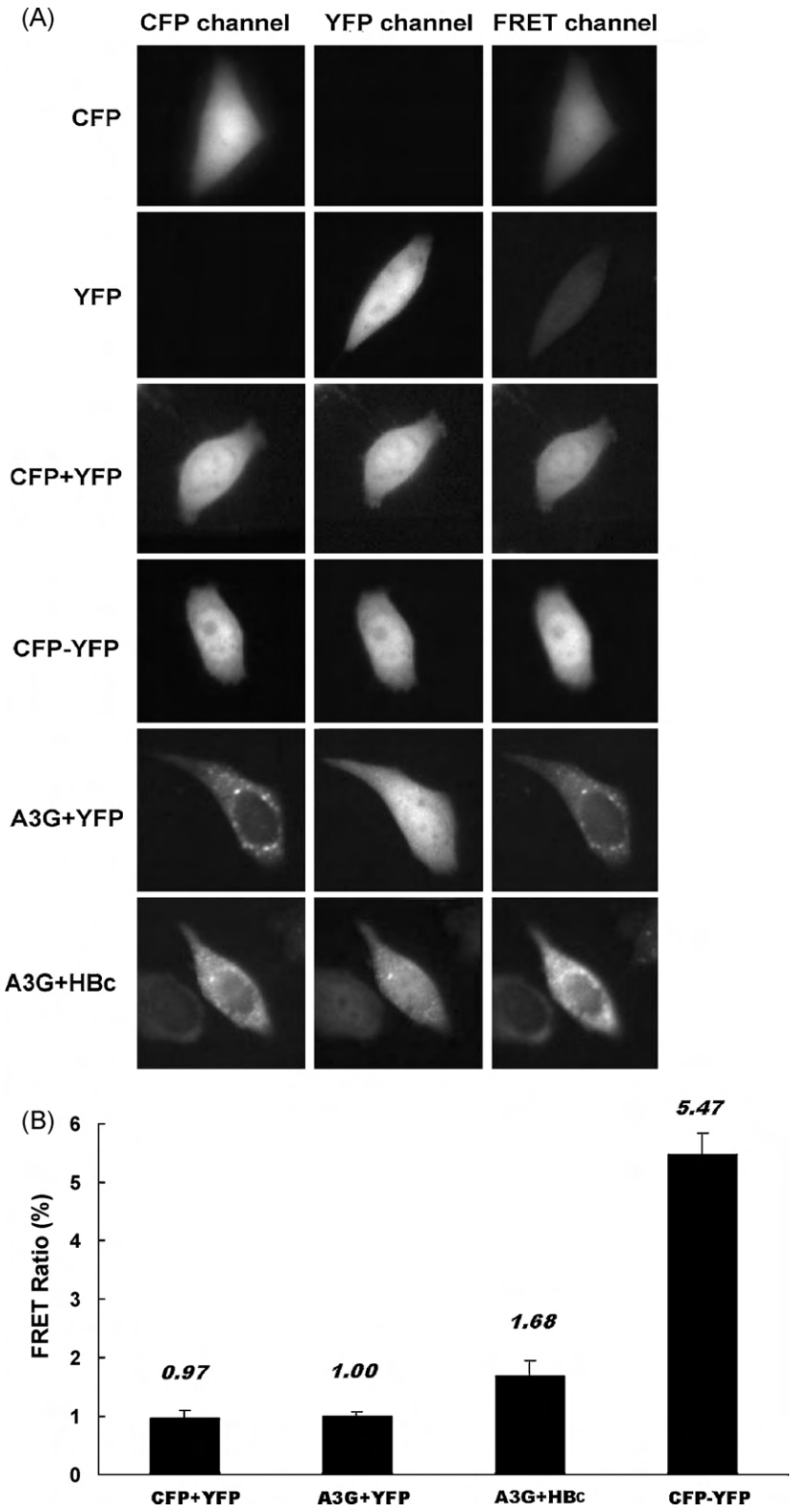

Fig. 2. Three-cube FRET revealed A3G and HBc interaction in living cells. (A) FRET imaging was used to visualize the interaction of A3G with HBc in living cells. The indicated CFP and YFP fusion proteins were expressed in HepG2 cells. Images were measured by the CFP channel (left column), YFP channel (middle column), and FRET channel (right column). (B) FRET efficiency was measured in the HepG2 cells co-expressing CFP and YFP or A3G and YFP (negative control), A3G and HBc, and CFP – YFP (positive control).

3.2. FRET revealed A3G and HBc interaction in living cells

To determine whether A3G interacted with HBc in living cells, the FRET approach was used. It is a sensitive and convenient way to report protein-folding mechanisms in living cells. To measure the steady-state of three-cube FRET, CFP or YFP was imaged using an epifluorescence microscopy through CFP, YFP and FRET filter channels. As expected, neither CFP nor YFP can be excited by 500 or 430 nm wavelength lights, but there was some signal in the FRET filter set (due to bleed-through of CFP/YFP). We removed this

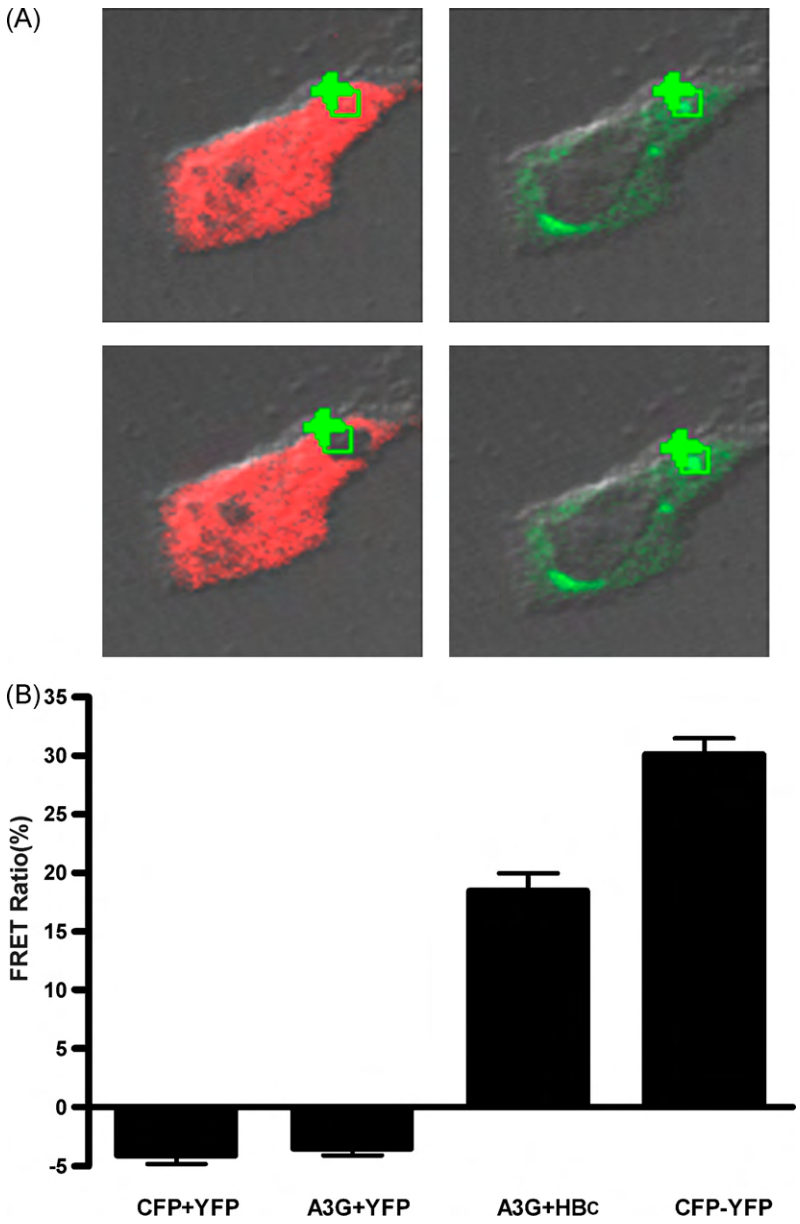

Fig. 3. FRET signal between A3G and HBc was detected using acceptor photobleaching. (A) Confocal fluorescence imaging of HepG2 cells co-transfected with A3G-CFP and HBc-YFP. Images in YFP (left) and CFP (right) channel were taken respectively before (top) and after (bottom) photobleaching YFP. The region of photobleach is indicated by the green outlined box. (B) Average FRET efficiency (%) was measured in CFP + YFP group (negative control), A3G + YFP, CFP – YFP group (positive control) and A3G-CFP + HBc-YFP group. FRET ratio was determined for the photobleached region in cytoplasm, whereas results showed the percentage of change in CFP after the photobleaching step. (For interpretation of the references to color in this figure legend, the reader is referred to the web version of the article.)

part of the signal in carrying out FRET calculations. To ensure the reliability of our recording system, we carried out some control experiments. First, cells co-expressing CFP and YFP that served as a negative control, and no FRET signal was observed (FR = 0.97 ± 0.02, n = 32). On the other hand, cells expressing the CFP–YFP concatemer, which served as a positive control, showed a significant FRET signal (FR = 5.47 ± 0.05, n = 49) (Fig. 2). Therefore, these control experiments verified that three-cube FRET provides sensitive and selective detection of FRET. Then we tested the interaction between A3G and HBc using the same system described above. We found that the FRET signal was produced from co-expression of A3G-CFP and HBc-YFP (FR = 1.68 ± 0.04, n = 52). We also co-transfected pA3G-CFP with pEYFP-N1 in HepG2 cells as a negative control. The FR value was 0.99 ± 0.01 (n = 61), similar to the result from the negative control. These results suggested that there was an interaction between A3G and HBc in living cells.

Acceptor photobleaching is another method of three-cube FRET measurement. When pECFP-N1 and pEYFP-N1 were co-transfected, the intensity of CFP was also reduced after bleaching YFP, so we were not able to measure any FRET. However, we measured a FRET efficiency (E_{EFF}, %) of 18.5 ± 2.4 (n = 28) in cytoplasm when A3G-CFP and HBc-YFP were co-expressed in HepG2 cells. In addition, FRET efficiencies (E_{EFF}, %) of 30.1 ± 1.4 (n = 18) were detected in pCFP–YFP transfected cells (positive control). No signal was detected in pA3G-CFP and pEYFP-N1 co-transfected group (Fig. 3).

3.3. BIAcore analysis of A3G/HBc interaction independent of RNA

Despite our FRET data indicated that A3G can interact with the HBc protein in HepG2 cells, the question of whether this interaction is dependent on either the presence of other proteins or post-translational modifications in cells is still unexplained. In order to

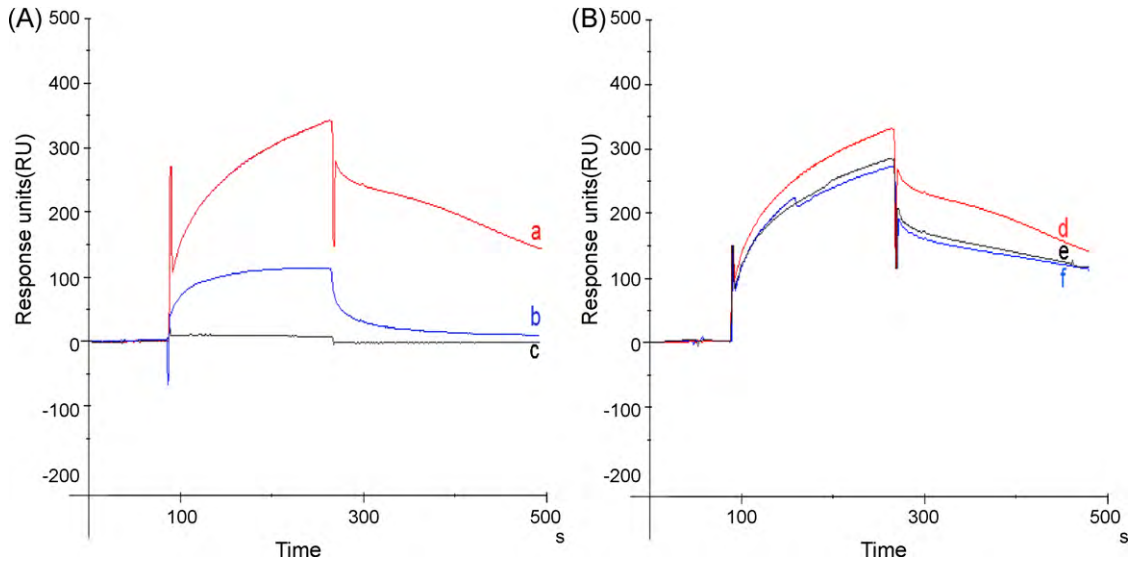

Fig. 4. BIAcore analysis of A3G/HBc interaction independent on RNA. (A) The binding of A3G and HBc was detected by Biacore assay. Curves a (red), b (blue), c (black) respectively represent the binding affinity of A3G, PGRN and HA-peptide with HBc. (B) The interaction of A3G and HBc was not enhanced by RNA. Total RNA of HepG2 or HepG2.2.15 cells was added to A3G protein solution before flow through the SPR chip, while the final concentration of RNA was 0.125 and 0.25 μg/μL, respectively. Curves d (red), e (black), and f (blue) respectively represent the binding affinity of HBc proteins with A3G, A3G that was added to HepG2 RNA, and A3G that was added to HepG2.2.15 RNA. (For interpretation of the references to color in this figure legend, the reader is referred to the web version of the article.)

answer this question, the direct interaction between A3G and HBc was first tested by SPR assay. Usually, HBc assembles into small and large icosahedral particles, so here we constructed an assembly defective mutant (pHBc-Y132A-HA) (Bourne et al., 2009). Proteins A3G-HA and HBc-Y132A-HA were purified by anti-HA antibody-conjugated agarose beads. As shown in Fig. 4A, there were no significant signals generated between the HBc-Y132A-HA and HA-peptide or the PGRN protein, while the interaction between A3G protein and HBc-Y132A-HA was detected. In order to examine the role of RNA in the interaction between them, we added the total RNA of HepG2 cells or HepG2.2.15 cells to the A3G protein solution before SPR analysis. As shown in Fig. 4B, the signal obtained from A3G and HBc-Y132A-HA was not affected when RNA of HepG2 or HepG2.2.15 cells was added. This suggested that RNA did not play a role in stabilizing the interaction.

4. Discussion

To the present, studies have detected that A3G can reduce the level of HBV transcripts and proteins and suppress HBV replication (Nguyen et al., 2007; Turelli et al., 2004). Also, some have shown that the anti-HBV activity of A3G may depend on its incorporation into the virus particle to inhibit reverse transcription (Baumert et al., 2007; Nguyen and Hu, 2008). However, how A3G is specifically packaged into HBV particle requires further investigation. By confocal fluorescence microscopy, we detected that A3G and HBc extensively co-localized in HepG2 cells. This suggested that A3G may interact with HBc in cytoplasm. To directly determine the interaction between them, we used both three-cube FRET measurement and acceptor photobleaching. The FRET signal was observed between A3G-CFP and HBc-YFP in HepG2 cells, and our findings strongly demonstrated that A3G can bind to HBc in the cytoplasm.

Recent studies have suggested that A3G can bind with cellular 7SL RNA, which promotes the interaction between A3G and GAG for viral incorporation (Bach et al., 2008; Wang et al., 2008a). Whether other cellular factors are required for the interaction between A3G and HBc protein remains unknown. The SPR approach is ideally suitable to study the protein–protein interaction *in vitro* and the possible effects of other cellular components can be eliminated (Nakajima et al., 2005). In this study, we first used the SPR approach and found direct physical interaction between HBc and A3G proteins in cell free systems. Cen et al. (2004) demonstrated that A3G binds to the HIV-1 Gag, but they also demonstrated that Gag/APOBEC3G complex is immunoprecipitated from cell lysate after RNase treatment. So we questioned whether HBV RNA or cellular RNA benefited from the interaction between A3G and HBc. We again used SPR to detect this relationship and certified that this binding was enhanced by neither the HepG2 cell RNA nor the HepG2.2.15 cell RNA. A possibility exists that the interaction is not dependent on RNA. These results are consistent with reports that the interaction between A3G and HIV-1 Gag is RNA-independent (Soros et al., 2007).

HBc is present in the nucleus and cytoplasm of infected hepatocytes. HBc can directly incorporate into the viral core that becomes the nucleus for reverse transcription upon infection of a cell. Schlicht et al. (1989) reported that the deletion of 36 amino acids from the carboxy terminus of the duck HBc abolished genome replication, although mutant cores formed capsid particles competent for genome packaging. Mutant proteins truncated to amino acid 163 or 164 packaged RNA but drastically reduced DNA synthesis (Nassal, 1992). These observations suggest that interactions with the HBc proteins can affect several steps in genome replication. Here we used different methods and certified that A3G can directly interact with HBc. This reveals that one of the mechanisms of A3G suppressing HBV DNA synthesis may be through binding core proteins directly.

In conclusion, we detected that A3G can bind HBc in both living cells and cell free systems. Our findings define a mechanism that A3G is incorporated into HBV nucleocapsids through binding the HBc protein. However, further studies are necessary to determine the interaction domains of A3G and HBc. Taken together, our results provide further insights into the inhibition of HBV replication by A3G. The binding sites in A3G proteins or HBc are attractive topics for the development of new antiretroviral agents. This investigation may facilitate the lead to progress in the making of a new approach for controlling HBV infection.

Acknowledgements

We thank Professor Luo Jian-hong for kindly supporting us by providing CFP–YFP plasmid and the three-cube FRET equipment. We also thank Gao Ying for her technological support and Mona Xiao for editorial assistance. This work was supported by Grant 30600519 from the National Natural Science Foundation of China and National Basic Research Program of China (973 Program, 2007CB512905) and 11th Five-year Special-purpose Program of China (2008ZX10002-007).

References

Aguiar, R.S., Peterlin, B.M., 2008. APOBEC3 proteins and reverse transcription. Virus Res. 134 (1–2), 74–85.
Alce, T.M., Popik, W., 2004. APOBEC3G is incorporated into virus-like particles by a direct interaction with HIV-1 Gag nucleocapsid protein. J. Biol. Chem. 279 (33), 34083–34086.
Bach, D., Peddi, S., Mangeat, B., Lakkaraju, A., Strub, K., Trono, D., 2008. Characterization of APOBEC3G binding to 7SL RNA. Retrovirology 5, 54.
Baumert, T.F., Rosler, C., Malim, M.H., von Weizsacker, F., 2007. Hepatitis B virus DNA is subject to extensive editing by the human deaminase APOBEC3C. Hepatology 46 (3), 682–689.
Bourne, C.R., Katen, S.P., Fulz, M.R., Packianathan, C., Zlotnick, A., 2009. A mutant Hepatitis B virus core protein mimics inhibitors of icosahedral capsid self-assembly (dagger). Biochemistry 48, 1736–1742.
Burnett, A., Spearman, P., 2007. APOBEC3G multimers are recruited to the plasma membrane for packaging into human immunodeficiency virus type 1 virus-like particles in an RNA-dependent process requiring the NC basic linker. J. Virol. 81 (10), 5000–5013.
Cen, S., Guo, F., Niu, M., Saadatmand, J., Deflassieux, J., Kleiman, L., 2004. The interaction between HIV-1 Gag and APOBEC3G. J. Biol. Chem. 279 (32), 33177–33184.
Chiu, Y.L., Greene, W.C., 2008. The APOBEC3 cytidine deaminases: an innate defensive network opposing exogenous retroviruses and endogenous retroelements. Annu. Rev. Immunol. 26, 317–353.
Douaisi, M., Dussart, S., Courcoul, M., Bessou, G., Vigne, R., Decroly, E., 2004. HIV-1 and MLV Gag proteins are sufficient to recruit APOBEC3G into virus-like particles. Biochem. Biophys. Res. Commun. 321 (3), 566–573.
Gao, Y., Liu, S.S., Qiu, S., Cheng, W., Zheng, J., Luo, J.H., 2007. Fluorescence resonance energy transfer analysis of subunit assembly of the ASIC channel. Biochem. Biophys. Res. Commun. 359 (1), 143–150.
Guarnieri, M., Kim, K.H., Bang, G., Li, J., Zhou, Y., Tang, X., Wands, J., Tong, S., 2006. Point mutations upstream of hepatitis B virus core gene affect DNA replication at the step of core protein expression. J. Virol. 80 (2), 587–595.
Harris, R.S., Bishop, K.N., Sheehy, A.M., Craig, H.M., Petersen-Mahrt, S.K., Watt, I.N., Neuberger, M.S., Malim, M.H., 2003. DNA deamination mediates innate immunity to retroviral infection. Cell 113 (6), 803–809.
Hu, J.L., Cui, J., Deng, X.Y., Zhang, W.L., Li, Q.L., Guo, J.J., Zeng, A.Z., Huang, A.L., 2009. A new strategy for constructing in vitro replication-competent 1.3 copies of hepatitis B virus genome. J. Virol. Methods 161 (1), 63–69.
Jarmuz, A., Chester, A., Bayliss, J., Gisbourne, J., Dunham, I., Scott, J., Navaratnam, N., 2002. An anthropoid-specific locus of orphan C to U RNA-editing enzymes on chromosome 22. Genomics 79 (3), 285–296.
Kao, J.H., Chen, D.S., 2002. Global control of hepatitis B virus infection. Lancet Infect. Dis. 2 (7), 395–403.
Karpova, T.S., Baumann, C.T., He, L., Wu, X., Grammer, A., Lipsky, P., Hager, G.L., McNally, J.G., 2003. Fluorescence resonance energy transfer from cyan to yellow fluorescent protein detected by acceptor photobleaching using confocal microscopy and a single laser. J. Microsc. 209 (Pt 1), 56–70.
Liao, W., Ou, J.H., 1995. Phosphorylation and nuclear localization of the hepatitis B virus core protein: significance of serine in the three repeated SPRRR motifs. J. Virol. 69 (2), 1025–1029.
Mangeat, B., Turelli, P., Caron, G., Friedli, M., Perrin, L., Trono, D., 2003. Broad antiretroviral defence by human APOBEC3G through lethal editing of nascent reverse transcripts. Nature 424 (6944), 99–103.
Nakajima, H., Cocquerel, L., Kiyokawa, N., Fujimoto, J., Levy, S., 2005. Kinetics of HCV envelope proteins' interaction with CD81 large extracellular loop. Biochem. Biophys. Res. Commun. 328 (4), 1091–1100.
Nassal, M., 1992. The arginine-rich domain of the hepatitis B virus core protein is required for pregenome encapsidation and productive viral positive-strand DNA synthesis but not for virus assembly. J. Virol. 66 (7), 4107–4116.
Nguyen, D.H., Gummuluru, S., Hu, J., 2007. Deamination-independent inhibition of hepatitis B virus reverse transcription by APOBEC3G. J. Virol. 81 (9), 4465–4472.
Nguyen, D.H., Hu, J., 2008. Reverse transcriptase- and RNA packaging signal-dependent incorporation of APOBEC3G into hepatitis B virus nucleocapsids. J. Virol. 82 (14), 6852–6861.
Ning, B., Shih, C., 2004. Nucleolar localization of human hepatitis B virus capsid protein. J. Virol. 78 (24), 13653–13668.
Schlicht, H.J., Bartenschlager, R., Schaller, H., 1989. The duck hepatitis B virus core protein contains a highly phosphorylated C terminus that is essential for replication but not for RNA packaging. J. Virol. 63 (7), 2995–3000.
Sells, M.A., Chen, M.L., Acs, G., 1987. Production of hepatitis B virus particles in Hep G2 cells transfected with cloned hepatitis B virus DNA. Proc. Natl. Acad. Sci. U.S.A. 84 (4), 1005–1009.
Sureau, C., Romet-Lemonne, J.L., Mullins, J.I., Essex, M., 1986. Production of hepatitis B virus by a differentiated human hepatoma cell line after transfection with cloned circular HBV DNA. Cell 47 (1), 37–47.
Soros, V.B., Yonemoto, W., Greene, W.C., 2007. Newly synthesized APOBEC3G is incorporated into HIV virions, inhibited by HIV RNA, and subsequently activated by RNase H. PLoS Pathog. 3 (2), e15.
Takanishi, C.L., Bykova, E.A., Cheng, W., Zheng, J., 2006. GFP-based FRET analysis in live cells. Brain. Res. 1091 (1), 132–139.
Turelli, P., Mangeat, B., Jost, S., Vianin, S., Trono, D., 2004. Inhibition of hepatitis B virus replication by APOBEC3G. Science 303 (5665), 1829.
Wang, S.M., Wang, C.T., 2009. APOBEC3G cytidine deaminase association with coronavirus nucleocapsid protein. Virology 388 (1), 112–120.
Wang, T., Tian, C., Zhang, W., Sarkis, P.T., Yu, X.F., 2008a. Interaction with 7SL RNA but not with HIV-1 genomic RNA or P bodies is required for APOBEC3F virion packaging. J. Mol. Biol. 375 (4), 1098–1112.
Wang, T., Zhang, W., Tian, C., Liu, B., Yu, Y., Ding, L., Spearman, P., Yu, X.F., 2008b. Distinct viral determinants for the packaging of human cytidine deaminases APOBEC3G and APOBEC3C. Virology 377 (1), 71–79.
Wedekind, J.E., Dance, G.S., Sowden, M.P., Smith, H.C., 2003. Messenger RNA editing in mammals: new members of the APOBEC family seeking roles in the family business. Trends Genet. 19 (4), 207–216.
Wichroski, M.J., Robb, G.B., Rana, T.M., 2006. Human retroviral host restriction factors APOBEC3G and APOBEC3F localize to mRNA processing bodies. PLoS Pathog. 2 (5), e41.
Zhang, L., Li, X., Ma, J., Yu, L., Jiang, J., Cen, S., 2008. The incorporation of APOBEC3 proteins into murine leukemia viruses. Virology 378 (1), 69–78.